A Study of Differences in Calculated Capacity when Using Single-, Mixed- or Multiple-Bounce GSCM Schemes

Radovan ZENTNER [1], Ana KATALINIĆ MUCALO [2], Robert NAĐ [1]

[1] University of Zagreb, Faculty of Electrical Engineering and Computing, Unska 3, 10000 Zagreb, Croatia
[2] Croatian Post and Electronic Communications Agency, Roberta Frangeša Mihanovića13, 10000 Zagreb, Croatia

radovan.zentner@fer.hr, ana.katalinic@hakom.hr, robert.nad@fer.hr

Abstract. *The paper looks for differences in MIMO system capacity when using either single-, mixed-, or multiple-bounce geometry based stochastic channel models (GSCMs). The investigation considers Saleh-Valenzuela temporal indoor model, expanded for angular domain. In the model omnidirectional and idealized sector antennas were used as array elements. The single-bounce assumption, combination of single and multiple bounces, and pure random multiple bounces assumption were compared within "temporally identical" environment regarding the overall MIMO capacity. Assumption of clustered scatterers/reflectors is used in all three cases. The comparison is performed in statistical sense, using a large number of stochastically generated temporal models. The model is two-dimensional, i.e. neither elevation angle nor polarization/ depolarization was considered.*

Keywords

Single-bounce, multiple-bounce, geometry stochastic channel model (GSCM), MIMO, indoor propagation.

1. Introduction

Stochastic channel models (SCM) [1] are important ingredient for practical evaluation of newly designed communication systems. They enable generation of numerous channel simulations, upon which performance of a system under development can be tested. To that goal, however, channel models must be adaptable for use with a specific system, coding scheme, modulation and topology (mobility, MIMO, multiple users, handover schemes, etc.).

Besides taking into account the need for adaptability, the designers of stochastic model are confronted with even more challenging question: is the model, and to which extent, realistic. While more realistic features are being added to the model, the model becomes more complex and difficult to use. Therefore every SCM is a trade off in which one needs to keep in mind the list of simplifications implemented in each model, test the impact of these simplifications, and reflect upon it when drawing general conclusions.

In that sense this paper aims in testing the difference when using single-, mixed-, or multiple-bounces assumption in the family of geometry-based stochastic channel models (GSCM) [1]-[4].

This investigation is unique in a sense that usually researchers either use single-bounce [5] or multiple-bounce [6], [7] assumptions, both suffering a simplification, former of ignoring rich multiple-bounces, and latter of ignoring the correlation between angle of arrival (AoA), angle of departure (AoD) and delay, present in single bounces. The difference between these three bouncing approaches is analyzed statistically, by running 80 times the same stochastic temporal model (thus obtaining 80 different realizations) and then comparing MIMO system capacities when applying different bounce schemes to these 80 realizations. Comparison for delay spread would be pointless since identical temporal model was used in all cases. This work focused on high-level practical consequences of using different bounce schemes. Investigation included validation across different antenna array elements, using idealized omni- and sector antennas. Also, validation of element spacing impact was performed.

The power, temporal and angular distributions of arriving rays around the receiver (Rx) are modeled using Saleh-Valenzuela-Spencer (SVS) model [8], [9]. This model is limited to single-input-multiple-output (SIMO) and multiple-input-single-output (MISO) and it was expanded in this paper to be applicable also for MIMO systems.

The paper is organized as follows. Section 2 gives description of SVS model and explains how we adapted this model to the full MIMO support. Section 3 introduces different ray bounce schemes to the model, and Section 4 explains methodology of comparison between model schemes by means of ergodic capacity. Section 5 presents comparison of performance for considered schemes.

2.   Description of the Model

Although the channels considered in the paper are symmetrical and antenna arrays of both sides can be used for both transmitting and receiving, for clarity of presentation one array will be labeled as transmitting (Tx) and the other as receiving (Rx) end. Thus AoDs are corresponding to angles of rays departing from Tx end and AoAs are corresponding to angles of rays arriving to the Rx end.

Parameter	symbol	value
Distance between Tx & Rx	r	20m
Standard deviation of AoAs within the cluster		24^0
Cluster arrival rate	Λ	1/(17 ns)
Ray arrival rate	λ	1/(5 ns)
Cluster decay constant	Γ	34 ns
Intracluster decay constant	γ	29 ns
Distance power law coefficient	α	3.5
Tx power	P_T	0 dBm
Noise floor	N	-110 dBm

Tab. 1. Parameters of the model, identical to those used in [9].

SVS model relies on the temporal model developed upon indoor measurements by Saleh and Valenzuela [8] and extended to SIMO i.e. MISO case by Spencer et al. [9].

The model separately treats temporal and spatial domains. Parameters used in this paper are parameters from the literature [9] listed in Tab. 1. The temporal domain is modeled as Poisson stochastic process. The angular distribution of rays around receiver (Rx) assumes uniform angular cluster distribution with Laplacian intracluster angular distribution of angles of arrival (AoAs).

This initial calculation for establishing ray properties around Rx comes directly from SVS model and is shown as top most box row in Fig. 1. Fig. 1 depicts new algorithm that enables, unlike SVS model alone, obtaining a MIMO channel realization of the model, its transfer matrix H and corresponding MIMO capacity.

Once the rays properties (power, delay, AoA) at the Rx are established (light green boxes in Fig. 1), the rays AoD are calculated according to the selected bounce scheme (yellow boxes in Fig. 1). Finally, antenna element distances are determined (2.5 or 4.0 cm), as well as Tx element patterns (omni, sector 180° or sector 120°), as noted in light red boxes in Fig. 1.

At a scattering point a uniformly distributed random phase of either 0° or 180° is offset to each ray. Initial temporal model [8] used continuously and uniformly distributed random phase between -180° and 180°, but we find it impractical since in this work wideband channel is analyzed. It is also physically just to assume only these two cases of phase shift (0 or 180°) at the scattering point. This approach has already been applied in [10].
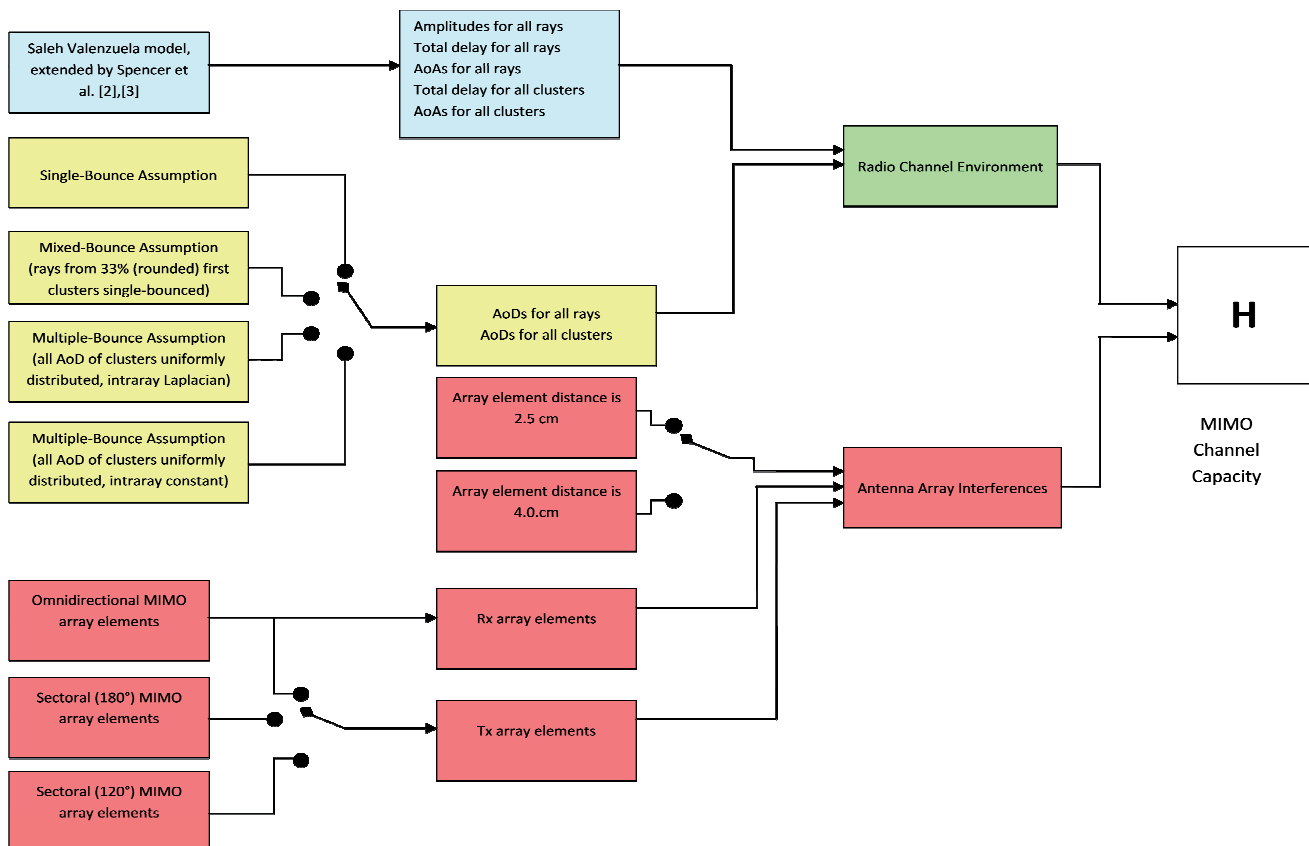

Fig. 1.   The block diagram of the model procedures for obtaining MIMO channel matrix.

Geometry model of the system was reduced to two dimensions, omitting the elevation angle as a parameter. The distance between Tx and Rx array locations was set to 20 m, and in case of directive antennas, the element radiation pattern was oriented in a way that line connecting Tx and Rx cuts the radiation pattern symmetrically, and pattern maxima were directed to each other. The antennas we applied at Tx were idealized omnidirectional antennas (with standard dipole gain of 2.15 dBi), and idealized sector antennas of either 180° or 120° of coverage. Sector antenna gains were higher than omnidirectional, adjusted to ensure their overall radiated power equals to the radiated power of omnidirectional antennas. Thus fair comparison for impact of reduced azimuth coverage could be performed. At the receiver side we used only omnidirectional antennas with 2.15 dBi gain.

For the purpose of investigation, a 3-element linear array at both ends (3 x 3 MIMO system) was considered, and capacity was calculated for an overall bandwidth from 3.25 to 3.90 GHz. The band was chosen so, because in related work [11] we considered real, non-idealized stacked patch antennas which operate in that frequency band. Regarding the distance between antenna array elements, two values were considered: 2.5 cm and 4.0 cm, for both Tx and Rx arrays. Further on, these arrays will be referred to as 2.5 cm arrays and 4.0 cm arrays, although their actual total lengths are 5 cm and 8 cm, respectively.

Fig. 2 shows geometry of all simulated cases. The element radiation (gain) patterns are shown symbolically, around the centre element of the array. All three types of Tx element patterns are shown: omnidirectional (solid line), 180° sector (dotted line) and 120° sector pattern (dashed line).
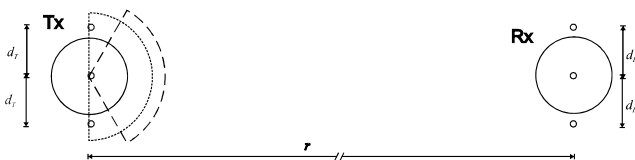

Fig. 2. Relative position of Tx and Rx antenna arrays with sketched considered element radiation patterns: omnidirectional antenna at Rx and 3 different radiation patterns at the Tx. Patterns are drawn around the centre element for clarity, but all array elements at each side had identical radiation pattern.

3. Modeling of Single-, Mixed- and Multiple-Bounces

Due to their simplicity, single bounce models [5], [12]-[13] are the first choice in GSCM. It is natural; the power of the ray that travels from Tx to Rx is significantly reduced each time it suffers a bounce, i.e. reflection, refraction or scattering. Still, it was found [7] that in rich scattering environments, such as indoors or street canyons, double and even triple bounced rays should be accounted

for. It is also found that ray-tracing algorithms converge only after third-order reflections are included [14].

There is a fundamental difference between single and multiple bounced rays: while in the case of single bounced rays the triplet of AoA, AoD and time delay are directly related to each other, such direct relation does not exist for multiple bounces. Our investigation is motivated by the question: is it appropriate to model all rays as multiple-bounced (as in [12], [15]) or will the fact that strongest rays are usually single-bounced cause a discrepancy between models and real scenarios.

We approached the problem indirectly, by comparing most popular bounce-management (BM) schemes and their combination. The comparisons were performed in statistical sense on all mentioned MIMO antenna array types, under 80 random temporal+AoA scenarios. Multiple-bounce clusters are modeled by uncoupling the AoA, AoD and time delay through independent generation of AoAs and AoDs.

The considered BM schemes are:

1. *Single-bounce (S-B) scheme* – all rays undergo only one reflection when traveling from Tx to Rx; AoA, power and time delay of rays are calculated using SVS model and AoD is than calculated geometrically from AoA and time delay, as elliptical model in [9].

2. *Mixed single- and multiple-bounce (Mix-B) scheme* - all rays belonging to the "first 33% clusters", i.e. with the shortest cluster time delay and of higher strength, in accordance to applied statistical model [8], [9], are kept single-bounced; for the remaining rays the multiple-bounce scheme under 3. is applied.

3. *Multiple-bounce (M-B) scheme* – AoDs are selected in the same manner as AoAs, i.e. AoD's cluster angle is chosen using uniform distribution around Tx, and intra-cluster distribution is again Laplacian, as in [9]. This model is inspired with twin-cluster model from [15].

4. *Multiple-bounce zero-intra-cluster-AoD-variation (keyhole) (Key-M-B) scheme* – same as under 3, except that there is no randomness in intracluster distribution for AoDs; all rays within the cluster have AoD equal to cluster's AoD.

The 4th scheme describes scenario in which the first bounce, after rays are launched from Tx, goes through a "strong keyhole-like" area. Due to the symmetry, this case has the same effect as the case where such a "keyhole-like" area appears as the last bounce before Rx. It is expected that for this scheme, on average, capacity is the lowest.

Fig. 3 illustrates these four schemes. There, average/typical values for AoAs and AoDs are graphically illustrated: in single bounce scheme angle spreads at Tx are different than at Rx; in mixed- and multiple-bounced schemes those clusters that are labeled as multiple-bounced have (on average) identical angular spreads, and finally, "keyhole" scheme has angular spread at Tx side reduced to zero.
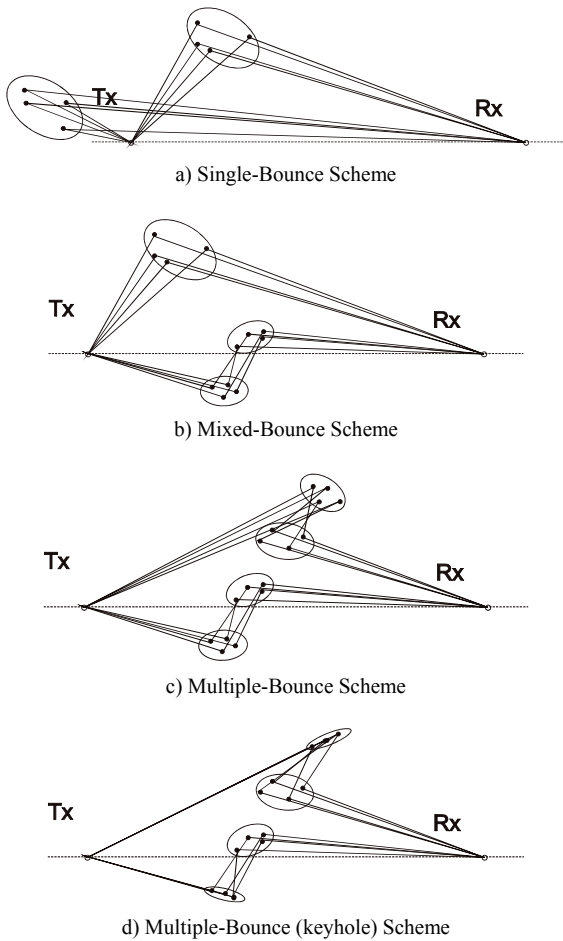
a) Single-Bounce Scheme

b) Mixed-Bounce Scheme

c) Multiple-Bounce Scheme

d) Multiple-Bounce (keyhole) Scheme

Fig. 3.   Illustration of four considered schemes.

4. MIMO Models and Ergodic Average Capacity Calculation

As mentioned above, 80 different temporal+AoA realizations were generated by SVS model as described before. For each of these realizations to describe a double-directional channel also AoD distribution is needed, which was generated according to each of four bounce schemes separately, as described above and in Fig. 3. Since for each of these ray-delay-AoA-profiles all 4 bounce schemes described in Sec. 3 were separately applied for AoD realizations calculation, total number of different generated environments is 320. In all of these environment realizations 3 types of antenna elements were used at Tx, and array element spacings were either 2.5 cm or 4.0 cm, at both Tx and Rx (4 element spacing combinations). Thus we dealt with 3x4 = 12 different antenna array combinations at air interfaces, i.e. 12 x 320 = 3840 different MIMO channels realizations were simulated in total. All channels were of dimension 3 x 3, and for each a capacity was calculated in the band of 3.25 GHz to 3.9 GHz.

For the calculation of MIMO capacity, the formula for maximal obtainable capacity without channel state information (CSI) at the transmitter [16] is used:

$$S_{\max} = \frac{C}{B} = \log_2\left[\det\left(I_m + \frac{SNR}{n} \cdot \mathbf{H} \cdot \mathbf{H}^* \right) \right] \qquad (1)$$

where n corresponds to the number of Tx and m to the number of Rx antennas, $\mathbf{I}$ denotes identity matrix, SNR denotes signal-to-noise ratio, $\mathbf{H}$ is MIMO transfer matrix in spectral domain and * denotes conjugate transpose of the matrix. C here denotes capacity and B the available bandwidth. Capacity was calculated in frequency domain, frequency by frequency, and for performance comparison an average capacity was used, which corresponds to total throughput divided by bandwidth.

The values presented here are average capacities within the bandwidth. Dependence of capacity upon frequency for one sample environment is shown in Fig. 4. This Rayleigh-like chart illustrates that 3-element array could not obtain sufficient angular resolution to distinguish all present rays individually (neither in reality this can be achieved due to small number of antennas), so that some rays are bundled together into beams. Each of these beams varies (Rayleigh-like) with frequency, since these "bundled" rays change their electrical lengths and sum up with different phase. Still, minima are much smaller than if it were (power-equivalent) ordinary Rayleigh/Rice distributed SISO case.
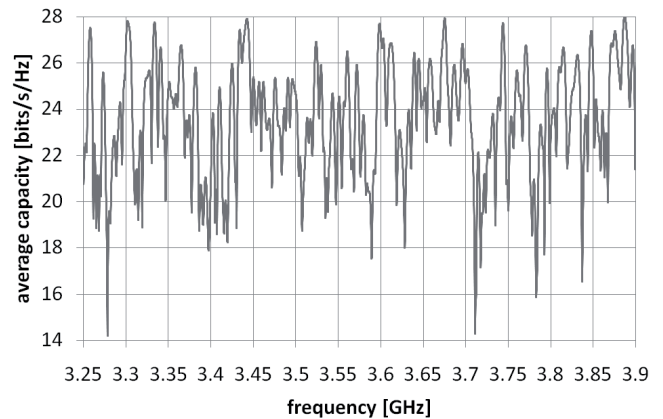

Fig. 4.   Illustration of capacity as a function of frequency.

5. Results

For the matter of easier presentation Tab. 2 lists all considered arrays at Tx or Rx and their type number that will be used further for labeling the arrays in the presentation of results.

Tab. 3 and 4 show the ergodic capacity, averaged within the band 3.25 to 3.9 GHz for MIMO systems with Rx array types 1 and 0, respectively. Only capacity with CSI at the receiver is considered. Identical 80 Temporal+AoA realizations were used for calculating ergodic capacity, and only AoDs distributions differed accordingly, dependent on the applied bounce scheme. Beside the ergodic capacity, its standard deviation is presented. It is worth noting that in spite of some deviation among reali-

zations, within same Temporal+AoA realization, the higher-lower-order for capacities of different bounce schemes corresponded in above 80% of realizations to the higher-lower-order of their corresponding ergodic capacities.

Array type	Array elements	Distance between elements
0	omnidirectional	4.0 cm
1	omnidirectional	2.5 cm
2	180^0 sector	4.0 cm
3	180^0 sector	2.5 cm
4	120^0 sector	4.0 cm
5	120^0 sector	2.5 cm

Tab. 2. Considered array types and their labels

Looking at the results, it can be noted that for omnidirectional array elements in all cases there is a small difference between S-B and M-B schemes.

For directional array elements the difference of M-B to S-B schemes becomes significant. Capacity for M-B case steadily decreases with increased directivity, since MIMO diversity is reduced as some rays are lost.

Capacity for S-B case steadily increases, since due to the fair-comparison conditions, the gain and ERP (effective radiated power) of directive antennas increases. This can be explained by the fact that we had Tx sector antennas directed towards Rx antennas, and by the fact that single-bounce assumption somewhat "focuses" available AoDs exactly in angle range where sector antennas are directed. Due to the same reason, if we would have directed our sector antennas away from Rx, the capacity would drop, compared to omnidirectional case.

The results in Tab. 3 and 4 for Mix-B scheme fall in between of results of S-B and M-B schemes, just as this scheme is created as a mix of these two schemes.

It can be also noted that scheme 4 (keyhole effect) in all charts yields lower capacity than schemes 1 and 2, and in many cases, the difference is significant. This behaviour is quite expected due to reduced number of uncorrelated paths.

One final remark: the increase of capacity for S-B cases due to more directional Tx antennas, while directed towards Rx antennas is not stabile. At certain angle of directivity the capacity would start to drop, due to the increasing number of multipath rays that get excluded due to the increased "blind angle range". This effect can already be observed in Tab. 4 where for arrays with 2.5 cm element distance the S-B ergodic capacity for 180° sector antennas still increases, compared to the omnidirectional case, but for 120° sector antenna array it decreases, comparing to their 180° sector antennas counterpart.

6. Conclusion

In this paper we investigated differences in radio channel modeling when applying different GSCM schemes, using calculated ergodic capacity as a measure of comparison. For this study we expanded Saleh-Valenzuela-Spencer indoor temporal+AoA model to the MIMO functionality and considered single-, mixed- and multiple-bounced environments, on 80 random realizations with different antenna topologies on both Tx and Rx end.

In total, we calculated capacity for 3840 different 3x3 MIMO channels. Results have shown systematic tenden-

Tx type (acc. to Tab.2)	Single-Bounce Scheme		Mixed Bounce Scheme		Multiple-Bounce Scheme		Multiple-Bounce (Keyhole) Scheme	
	Ergodic Capacity (EC) [bits/s/Hz]	EC's standard deviation [bits/s/Hz]	Ergodic Capacity (EC) [bits/s/Hz]	EC's standard deviation [bits/s/Hz]	Ergodic Capacity (EC) [bits/s/Hz]	EC's standard deviation [bits/s/Hz]	Ergodic Capacity (EC) [bits/s/Hz]	EC's standard deviation [bits/s/Hz]
Type 0 (omnidir., d = 4.0 cm)	23,71	2,15	23,58	2,29	23,28	2,41	22,33	3,02
Type 1 (omnidir., d = 2.5 cm)	22,50	2,09	22,36	2,32	22,56	2,33	21,86	2,78
Type 2 (180^0, d = 4.0 cm)	25,73	2,29	25,16	2,63	22,03	3,32	19,92	4,11
Type 3 (180^0, d = 2.5cm)	24,30	2,26	23,75	2,66	21,45	3,13	19,55	3,95
Type 4 (120^0, d = 4.0 cm)	26,44	2,55	25,67	2,83	21,47	3,94	17,62	5,40
Type 5 (120^0, d = 2.5 cm)	24,36	2,44	23,58	2,74	19,92	3,68	16,69	4,96

Tab. 3. Ergodic capacity of considered MIMO systems and schemes (in bits/s/Hz) averaged over 80 temporal environment random runs, averaged within the band 3.25 to 4.0 GHz, for all considered Tx array types and Rx array type 1 (omnidirectional antenna elements at distance d = 2.5 cm)

Tx type (acc. to Tab.2)	Single-Bounce Scheme		Mixed Bounce Scheme		Multiple-Bounce Scheme		Multiple-Bounce (Keyhole) Scheme	
	Ergodic Capacity (EC) [bits/s/Hz]	EC's standard deviation [bits/s/Hz]	Ergodic Capacity (EC) [bits/s/Hz]	EC's standard deviation [bits/s/Hz]	Ergodic Capacity (EC) [bits/s/Hz]	EC's standard deviation [bits/s/Hz]	Ergodic Capacity (EC) [bits/s/Hz]	EC's standard deviation [bits/s/Hz]
Type 0 (omnidir., d = 4.0 cm)	24.36	2.13	24.35	2.24	24.14	2.38	23.05	3.08
Type 1 (omnidir., d = 2.5 cm)	23.18	2.27	23.15	2.44	23.33	2.32	22.52	2.82
Type 2 (180^0, d = 4.0 cm)	25.94	2.26	25.72	2.45	22.88	3.48	20.58	4.39
Type 3 (180^0, d = 2.5cm)	24.48	2.45	24.32	2.68	22.19	3.25	20.14	4.20
Type 4 (120^0, d = 4.0 cm)	26.30	2.48	26.00	2.61	22.37	4.21	18.24	5.71
Type 5 (120^0, d = 2.5 cm)	24.06	2.50	23.82	2.67	20.70	3.95	17.20	5.22

Tab. 4. Ergodic capacity of considered MIMO systems and schemes (in bits/s/Hz) averaged over 80 temporal environment random runs, averaged within the band 3.25 to 4.0 GHz, for all considered Tx array types and Rx array type 0 (omnidirectional antenna elements at distance d=4.0 cm).

cies and major differences in calculated capacities for 4 schemes that were considered.

Due to the fact that the use of directional sector antennas at base-station side is quite likely in many applications of MIMO systems, results obtained for S-B, M-B and Key-M-B schemes with these antenna types at Tx are very important. Based on these results, we can address the question whether all rays could be modeled as multiple-bounced (for simplicity) or should single-bounced rays be modeled as well, and incorporated into model for example in a way proposed in this paper as a Mix-B scheme. The results suggest that in order to implement directional antennas for GSCM of different scenarios, the process of measurement, parameterization and modeling should detect and estimate accurate portions of both S-B and M-B rays, which could then be implemented jointly in the model according to suggested Mix-B scheme.

References

[1] ALMERS, P. et al. Survey of channel and radio propagation models for wireless MIMO systems. *EURASIP Journal on Wireless Communications and Networking*, 2007, article ID 19070, 19 p.

[2] HANEDA, K., POUTANEN, J., TUVFESSON, F., LIU, L., KOLMONEN, V., VAINIKAINEN, P., OESTEGES, C. Development of multi-link geometry-based stochastic channel models. In *Antennas and Propagation Conference (LAPC 2011)*. Loughborough (UK), 14-15 November 2011, p. 1-7.

[3] VERDONE, R., ZANELLA, A. Pervasive mobile and ambient wireless communications. *COST Action 2100 (Signals and Communication Technology)*, Springer, 2012.

[4] POUTANEN, J., HANEDA, K., LINGFENG LIU, OESTEGES, C., TUFVWSSON, F., VAINIKAINEN, P. Parameterization of the COST 2100 MIMO channel model in indoor scenarios. In *Proceedings of the 5th European Conference on Antennas and Propagation (EUCAP)*. Rome (Italy), 11-15 April 2011, p. 3606-3610.

[5] RAPPAPORT, T. S., LIBERTI, J. C. *Smart Antennas for Wireless Communications*. Chapter 7. Upper Saddle River (NJ, USA): Prentice Hall PTR, 1999.

[6] KUIPERS, B. W. M., MACKOWIAK, M., CORREIA, L. M. Understanding geometrically based multiple bounce channel models. In *The Second European Conference on Antennas and Propagation*, *EuCAP 2007*. p. 1–4

[7] OESTEGES, C. Multi-link propagation modeling for beyond next generation wireless. In *Antennas and Propagation Conference (LAPC 2011)*. Loughborough (UK), 14-15 November 2011, p. 1-8.

[8] SALEH, A. A. M., VALENZUELA, R. A. A statistical model for indoor multipath propagation. *IEEE Journal on Selected Areas in Communications*, February 1987, vol. 5, no. 2.

[9] SPENCER, Q. H., JEFFS, B. D., JENSEN, M. A., SWINDLEHURST, A. L., Modeling the statistical time and angle of arrival characteristics of an indoor multipath channel. *IEEE Journal on Selected Areas in Communications*, March 2000, vol. 18, no. 3.

[10] FOERSTER, J., LI, Q. UWB channel modeling contribution from Intel. *IEEE P802.15 Working Group for Wireless Personal Area Networks (WPANs), IEEE P802.15-02/279r0-SG3a*, June 2002, p. 21-22.

[11] ZENTNER, R., KATALINIĆ A., NAGY, R., Geometry based stochastic analysis of MIMO channel performance when using stacked microstrip antennas. In *The Third European Conference on Antennas and Propagation, EuCAP 2009*.

[12] CORREIA, L. (Ed.) *Mobile Broadband Multimedia Networks, COST 273 final report. Elsevier Science Publishers B.V.*, 2006.

[13] MARQUES, G., CORREIA, L. M. A wideband directional channel model for mobile communication Systems. In S. Chandran (ed.), *Adaptive Antenna Arrays*, Berlin, (Germany): Springer, 2004.

[14] FOSCHINI, F. et al. Analysis of multipath propagation in urban environment through multidimensional measurements and advanced ray tracing simulation. *IEEE Transactions on Antennas and Propagation*, vol. 56, no. 3, March 2008, pp. 848 – 857

[15] HOFSTETTER, H., MOLISCH, A., CZINK, N. A twin-cluster MIMO channel model. In *The First European Conference on Antennas and Propagation, EuCAP 2006.* p. 1 – 4

[16] FOSCHINI, G. J., GANS, M. J. On limits of wireless communications in a fading environment when using multiple antennas. *Wireless Personal Communications*, 1998, vol. 6, p. 311 to 335.

About Authors …

Radovan ZENTNER graduated electrical engineering at University of Zagreb in 1994. Since 1995 he served as a research assistant at University of Zagreb where he also received his Ph. D. in 2002 (with honors). His research focus is on radio channel modeling for MIMO systems, broadband microstrip antennas and arrays, multiple antenna schemes for wireless communications and heuristic optimization techniques (genetic algorithms). He published more than 30 scientific papers in journals and conference proceedings. He participated in several European Union funded projects in antennas (COST 260, COST 284) and wireless communications (COST 273, COST 2100). Since 2011, he is an appointed management committee member of COST IC1004 project: Cooperative Radio Communications for Green Smart Environments. He holds the associate professor position at University of Zagreb, Faculty of Electrical Engineering and Computing. He is a member of IEEE, and has served as Joint AP-MTT Chapter Chair of Croatia Section. Currently, he serves as AP Chapter Chair of Croatia Section.

Ana KATALINIĆ MUCALO graduated electrical engineering at University of Zagreb in 2005. Since graduation she has been with Radiocommunications Department at Croatian Post and Electronic Communications Agency (HAKOM) as an Expert for Microwave and Satellite Networks, dealing mostly with frequency planning and interference analysis of fixed point-to-point and satellite links, as well as with cross-border coordination for fixed networks. She is also engaged in work of CEPT working group SE (Spectrum Engineering), which deals with compatibility studies and development of sharing criteria between different radio communication services and provides technical background for ECC decisions and recommendations. Her research interest is related to radio channel modeling for MIMO wireless systems, focusing especially on dynamic multipath effects, visibility regions parameterization and implementation of mobility. Currently, she is preparing her PhD thesis on Deterministic Radio Channel Modeling. She has published several scientific papers in conference proceedings and participated in European Union funded project for wireless communications COST2100. She is IEEE member.

Robert NAĐ is a full professor at the Department for Wireless Communications, received the B.S., M.S. and Ph.D. degrees in Electrical Engineering from the University of Zagreb, Croatia, in 1974, 1980 and 1993, respectively. The theme of his M.Sc. was "Work analysis of aligned amplifiers on high frequencies using S parameters" and his Ph.D. "Influence of passive network semiconductors amplifier small signal on work in predefined range of amplitudes and frequencies". He is a member of IEEE and KoREMA. He is also a member of technical committee DZNM/E TO 102. He is the author of more than 60 scientific papers in journals and conferences and numerous internal reports.